Orientation dependence of the carbon K edge in graphite measured by reflection electron-energy-loss spectroscopy

T. T. P. Cheung
Phillips Research Center, Phillips Petroleum Company, Bartlesville, Oklahoma 74004
(Received 19 November 1984)

The orientation dependence of the core electron-energy loss of the carbon K edge in highly oriented pyrolytic graphite has been examined as a function of θ, the angle between the incident electron beam and the c axis normal to the basal plane of the graphite. The energy-loss spectra, detected in the reflection mode with a cylindrical mirror analyzer, show two major losses at 284.9 and 291.6 eV, corresponding, respectively, to the transition to the π and σ conduction band. The π loss has an angular dependence of $(A+B\cos^2\theta)$ while the σ loss has a dependence of $(C-D\cos^2\theta)$, where the coefficients A, B, C, and D are all positive. The angular dependence of the σ loss cannot be explained without including the contribution from the monopole transition from the C($1s$) level to the $2s$ component of the sp^2 orbitals of the σ band, thus indicating the breakdown of the dipole selection rule. The difference spectrum between two orientations shows that there is a second but weaker transition in the π loss at 287.2 eV. The line shape of the π loss is interpreted in terms of the configuration interaction between the core exciton (at $\sim$285 eV) with the π conduction states. The energy loss at 287.2 eV is assigned to the direct transition to the saddle point Q_{2g} in the π band.

I. INTRODUCTION

In this paper, we report the orientation dependence of the core electron-energy loss (CEEL) of the carbon K edge in highly oriented pyrolytic graphite (HOPG). The CEEL line shapes were measured in the reflection mode as a function of the angle θ between the incident electron beam and the c axis normal to the basal plane of the graphite using a cylindrical mirror analyzer (CMA) as the detection device.

This study is spurred by the growing popularity of adapting commercial Auger spectrometers to do CEEL.[1–5] There are two major concerns involving reflection CEEL. First, materials with anisotropic electronic properties may have CEEL line shapes depending on the orientation of the anisotropy axis with respect to the excitation beam. Although detectors like the CMA provide some sort of averaging over the momentum space, the averaging is rather restricted and does not remove the angular dependence. Second, the validity of the dipole selection rule for the transition matrix elements is questionable. In transmission experiments where high-energy electron beams (10 keV or higher) are used, electrons scattered at or near the forward direction are measured. In this low-momentum-transfer limit, the transition matrix elements obey the same dipole selection rule[6] as in x-ray absorption except that the polarization vector in the optical case is replaced by the momentum-transfer vector. On the other hand, in the reflection experiments much weaker electron beams are employed and the backscattered electrons suffer large momentum transfer. In such conditions, the breakdown[6] of the dipole selection rule is not unexpected. There will be transition intensities resulting from excitations to optical forbidden final states. One can follow the forbidden transitions in reflection experiments by varying the excitation beam energies[7,8] or in transmission experiments by detecting electrons with large momentum transfer.[9–11] In this paper, we shall show that the breakdown of the dipole selection rule can also be identified by studying the angular dependence of the line shapes.

Orientation dependences of CEEL spectra have been investigated by Leapman and Silcox[12] in transmission mode. They measured the line shape of boron nitride, which has a hexagonal lattice similar to that of graphite, as a function of the momentum transfer in two different orientations. Orientation dependence has also been observed in the secondary electron emission from graphite.[13] Here, the transitions are between the valence and the conduction bands.

Studies of the CEEL line shape may also provide information about the electron density of states above the Fermi level E_f, provided that the independent-particle picture holds. In reality, the line shape is often complicated by the final-state effects induced by the core hole. A case in point is the carbon K edge in graphite.[14] Results of Mele and Ritsko indicated a drastic distortion of the density of states of the empty π band because of the core-excitonic effects. However, a weak transition has recently been observed[1,3] near the location corresponding to the maximum of the π density of states above E_f. The origin of this transition remains unclear. By subtracting spectra of different orientations, we shall show that the weak transition is associated with the π band. Its origin will be discussed. We shall summarize the details of the experiments in next section, and the results and discussion will be given in Sec. III.

II. EXPERIMENTAL AND MATERIALS

The CEEL data were measured using a Perkin-Elmer PHI-550 electron spectroscopy for chemical analysis

 ©1985 The American Physical Society

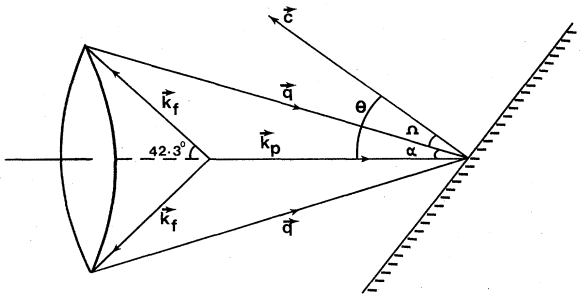

FIG. 1. Scattering geometry in reflection-core electron-energy-loss spectroscopy using cylindrical mirror analyzer (CMA) for detection. The wave-vector of the incident beam, $\mathbf{k}_p$, is coaxial with the CMA.

(ESCA)/Auger electron spectrometer equipped with an electron gun coaxial to the double pass cylindrical mirror analyzer (CMA). An excitation beam with an energy $E_p = 500$ eV and a current less than 1 μA was used. The surface of the acceptance cone for the backscattered electrons comprises an angle of 42.3° with respect to the axis of the CMA, thus to the direction of the excitation beam. For $E_p = 500$ eV and an energy loss of ~ 285 eV, the momentum transfer $q \equiv |\mathbf{q}|$ is about 17.8 Å^{-1}, where $\mathbf{q} = \mathbf{k}_p - \mathbf{k}_f$, with $\mathbf{k}_p$ and $\mathbf{k}_f$ being, respectively, the wave-vector of the incident electrons and the backscattered electrons. The details of the scattering geometry are given in Fig. 1. It should be noted that q remains fixed as θ varies.

Spectra were obtained in the derivative mode, $d(EN(E))/dE$, with a 0.5-V peak-to-peak modulation amplitude using lock-in detection. The energy resolution $\Delta E/E$ of the CMA was set at 0.6%.

The HOPG crystals (x-ray monochromator grade) were obtained from Union Carbide in a size of $10 \times 10 \times 2$ mm^3. They were freshly cleaved by the standard peeling technique prior to insertion into the ultrahigh vacuum chamber. Data were collected when the analysis chamber reached a pressure $\sim 2 \times 10^{-9}$ Torr. The orientation of the c axis of the HOPG crystal with respect to the CMA axis was accurate within $\pm 2°$. For each orientation, a freshly cleaved crystal was used to avoid prolong exposure to the excitation beam. Spectra were monitored throughout the data acquisition to check for possible changes due to radiation damage. Also, since the beam spot was less than 0.5 mm in size, spectra at several different locations of the same sample were taken to check for consistency. In all cases, spectra were well reproduced and there were no signs of radiation damage.

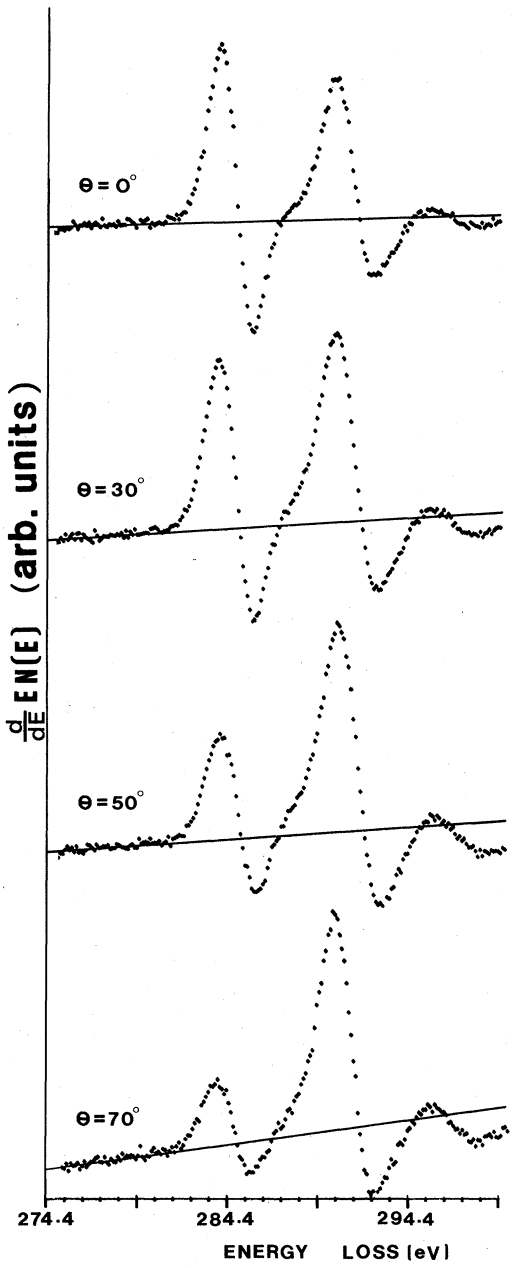

FIG. 2. Orientation dependence of the core electron-energy-loss spectra (given in $d[EN(E)]/dE$) of the highly oriented pyrolytic graphite as a function of θ, the angle between the incident electron beam and the c axis normal to the basal plane of the graphite.

III. RESULTS AND DISCUSSION

The CEEL spectra of HOPG at different values of θ are shown in Fig. 2. For the sake of clarity, the intensity of each spectrum is scaled differently to a fixed maximum-to-minimum separation. The energy losses at 284.9 and 291.6 eV, as determined from the numerically integrated spectra, are in general agreement with the results of others in reflection[1,3,4] and transmission[15,16] experiments as well as in x-ray absorption measurements.[17] Some have claimed[1,3] that these transitions correspond, respectively, to the initial electron density of states of the π and σ conduction bands. However, from the peak shape and detailed comparison with the calculated density of states, Mele and Ritsko[14] suggested that, for the energy loss at 285 eV, the transition is due to the excitation of the $C(1s)$ electron to the core-excitonic state arising from the π conduction band. Therefore, it does not necessarily re-

flect the initial density of states of the π band. Regardless of the interpretation, it is certain that the losses at 285 and 292 eV are due to the excitation of the $C(1s)$ electron to the π and σ conduction band, which for convenience, we shall refer to them as the π loss and the σ loss.

From Fig. 2, one may observe the large changes in the relative intensities between the π loss and the σ loss as a function of θ. At $\theta=0°$, the π loss is more intense than the σ loss. As θ increases, the π loss is reduced in comparison to the σ loss. Finally, at large θ, the σ loss dominates the spectrum. In order to follow the changes in the intensities as a function of θ, the spectrum at each orientation is normalized with respect to the intensity of the elastic peak measured under the same experimental conditions. Since q is fixed, the line shape of each *individual* transition in the CEEL spectrum should be independent of θ. Therefore in the derivative spectrum, the normalized peak height above the background (i.e., the normalized distance from the top of the positive peak to the background) is proportional to the intensity of that transition. The background is determined by fitting the low-energy-loss region of the spectrum by a straight line (see Fig. 2). We shall denote the normalized peak height of the π loss and σ loss, respectively, by $P(\theta)$ and $S(\theta)$. In Fig. 3, we plot $P(\theta)/P(\theta=0)$ and $S(\theta)/S(\theta=0)$ as a function of $\cos^2(\theta)$. Clearly, the θ dependence can be represented by

$$P(\theta)/P(\theta=0)=A+B\cos^2(\theta)\ , \tag{1}$$

and

$$S(\theta)/S(\theta=0)=C-D\cos^2(\theta)=(C-D)+D\sin^2(\theta)\ , \tag{2}$$

with $A=0.1$, $B=0.9$, $C=1.3$, and $D=0.3$.

The dipole selection rule may explain the orientation dependence of the π loss, although, as shall be shown below, it fails for the σ loss. Within the dipole approximation, the matrix element for the transition from the spherical $C(1s)$ orbital to the π band is nonzero when $\mathbf{q}$ has a component parallel to c axis. For transitions to the σ band, only transitions to the p_x and p_y components of the sp^2 orbitals are optically allowed, and the matrix element is nonzero when $\mathbf{q}$ has a component perpendicular to the c axis. Calculations [see Eqs. (7) and (10) below] show that the intensities of the π loss and σ loss vary, respectively, as $\cos^2\Omega$ and $\sin^2\Omega$, where Ω is the angle between $\mathbf{q}$ and the c axis. According to Fig. 1, the CMA will accept Ω within the range of $|\theta-\alpha|$ and $(\theta+\alpha)$, where α is the angle between $\mathbf{k}_p$ (i.e., the axis of the CMA) and $\mathbf{q}$. In the present case where the acceptance cone of the CMA sustains 42.3° with respect to $\mathbf{k}_p$, we have $\alpha=16.5°$. Let ϕ be the azimuth angle of $\mathbf{q}$ projected onto the plane perpendicular to $\mathbf{k}_p$. Now using the expansion

$$\cos(\Omega)=\cos(\alpha)\cos(\theta)+\sin(\alpha)\sin(\theta)\cos(\phi) \tag{3}$$

and averaging ϕ from 0 to 2π, we obtain, with $\alpha=16.5°$,

$$P'(\theta)/P'(\theta=0)=0.04+0.96\cos^2\theta\ , \tag{4}$$

and

$$S'(\theta)/S'(\theta=0)=12.0-11.0\cos^2\theta\ . \tag{5}$$

The prime designates the dipole approximation. One should note that the averaging of ϕ from 0 to 2π is correct only when θ is smaller than 47.7° because when $\theta>47.7°$, part of the acceptance cone of the CMA is blocked by the sample surface. However, the error resulting from the incomplete averaging of ϕ is negligible for $\theta\sim50°$. It remains small even when $\theta>50°$.

The dipole selection rule explains the drastic reduction of the intensities of the π loss as θ goes from 0° to 70°. It gives correctly the slope B of the experimental curve $P(\theta)/P(\theta=0)$ and, by a factor of 2, the intercept A (at $\theta=90°$). As for the σ loss, it predicts increases in the intensity as θ increases, as would be expected from a $\sin^2\theta$ dependence. However, Figs. 2 and 3 show that the σ loss does not vary to the same extent as the π loss. In particular, contrary to the expectation that the σ loss should be strongly suppressed at $\theta=0°$, it remains as strong as the π loss. Comparing Eqs. (2) and (5), one observes that the dipole selection rule gives the completely wrong slope and intercept. They are off by an order of magnitude!

This discrepancy is due to the breakdown of the dipole selection rule in the large-momentum-transfer regime. As mentioned in Sec. II, the momentum transfer q is as large as 17.8 Å^{-1}. Since the effective size of the $C(1s)$ orbital r_0 is of the order of one sixth of a Bohr radius, therefore $qr_0\sim1.6$. Clearly, the condition for the dipole approximation, $qr_0\ll1$, is violated. Now, the monopole transition from the $C(1s)$ level to the $2s$ component of the sp^2 orbitals of the σ band is no longer forbidden. This dipole-forbidden transition is independent of the angle Ω, thus also θ. Therefore the σ loss remains intense even at $\theta=0°$.

In order to gain further insight about the breakdown of the dipole selection rule, and about the coefficient C and D in Eq. (2), we examine the transition matrix M_q more carefully. For the σ loss,

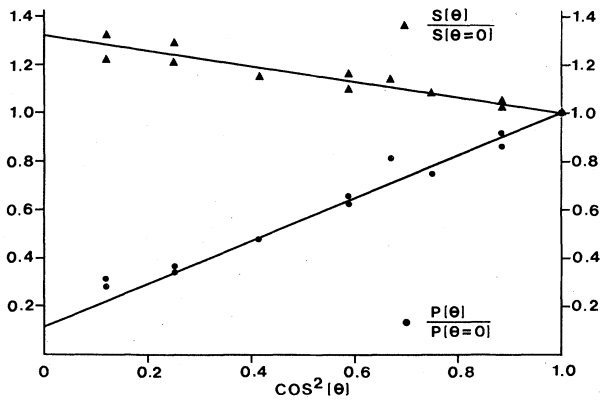

FIG. 3. Changes in the intensities of the π loss (at 285 eV), $P(\theta)/P$ ($\theta=0°$), and the σ loss (at 292 eV), $S(\theta)/S$ ($\theta=0°$), as a function of $\cos^2(\theta)$.

$$M_q(1s\rightarrow\sigma)=|\langle 1s|\exp(i\mathbf{r}\cdot\mathbf{q})|\sigma\rangle|^2$$
$$=|\langle 1s|\exp(i\mathbf{r}\cdot\mathbf{q})\times\{a|2s\rangle+b|2p_{-1}\rangle+c|2p_{+1}\rangle\}/\sqrt{3}|^2 , \quad (6)$$

where the coefficients a, b, and c have a modulus of unity. The second equality follows from the fact that the spatial range of $|1s\rangle$ is very small. The major contribution to M_q is therefore from the overlap between $|1s\rangle$ and that part of the $|\sigma\rangle$ representing the atomic orbitals localized on the same atom. Expanding $\exp(i\mathbf{r}\cdot\mathbf{q})$ in terms of the spherical harmonic Y_l^m and the spherical Bessel function j_l gives

$$\exp(i\mathbf{r}\cdot\mathbf{q})=\sum_{l=0}^{\infty}\sum_{m=-l}^{l}4\pi i^l j_l(qr)Y_l^{m*}(\mu,\nu)Y_l^m(\Omega,\Phi) ,$$

where (μ,ν) and (Ω,Φ) are, respectively, the polar angles of $\mathbf{r}$ and $\mathbf{q}$ with respect to the c axis. Then integration over μ, ν, and Φ leads to

$$M_q(1s\rightarrow\sigma)=\xi/3+v\sin^2(\Omega) , \quad (7)$$

with

$$\xi=\left[\int_0^{\infty}r^2drR_{1s}(r)j_0(qr)R_{2s}(r)\right]^2 ,$$
$$v=\left[\int_0^{\infty}r^2drR_{1s}(r)j_1(qr)R_{2p}(r)\right]^2 .$$

$R_{1s}(r)$ and $R_{2p}(r)$ are, respectively, the radial functions of the $1s$ and $2p$ orbitals. The monopole and dipole contributions are given respectively by ξ and v. Substituting in Eq. (3) and integrating over ϕ, we have

$$\langle\langle M_q(1s\rightarrow\sigma)\rangle\rangle=\{\xi/3+v[1-(\tfrac{1}{2})\sin^2\alpha]\}$$
$$-v[\cos^2\alpha-(\tfrac{1}{2})\sin^2\alpha]\cos^2\theta , \quad (8)$$

and

$$S(\theta)/S(\theta=0)=\langle\langle M_q(1s\rightarrow\sigma)\rangle\rangle/\langle\langle M_q(1s\rightarrow\sigma)\rangle\rangle|_{\theta=0}$$
$$=[\lambda/3+1-(\tfrac{1}{2})\sin^2\alpha]/[\lambda/3+1-\cos^2\alpha]-\{[\cos^2\alpha-(\tfrac{1}{2})\sin^2\alpha]/[\lambda/3+1-\cos^2\alpha]\}\cos^2\theta , \quad (9)$$

with

$$\lambda=\xi/v=\left[\int_0^{\infty}r^2drR_{1s}(r)j_0(qr)R_{2s}(r)\right]^2\Big/\left[\int_0^{\infty}r^2drR_{1s}(r)j_1(qr)R_{2p}(r)\right]^2 .$$

Here $\langle\langle\ \rangle\rangle$ denotes the averaging over ϕ. The coefficients C and D can be determined by comparing Eq. (2) with Eq. (9). They are mainly governed by λ, the ratio of the monopole transition to the dipole transition. Using $\alpha=16.5°$ and the experimental C and D, we find, for $q=17.8$ Å^{-1}, $\lambda\sim 8$.

Similarly, we obtain

$$M_q(1s\rightarrow\pi)=3v\cos^2\Omega , \quad (10)$$

and

$$\langle\langle M_q(1s\rightarrow\pi)\rangle\rangle$$
$$=(\tfrac{3}{2})v\sin^2\alpha+3v[\cos^2\alpha-(\tfrac{1}{2})\sin^2\alpha]\cos^2\theta . \quad (11)$$

As would be expected, one recovers the dipole selection rule from Eqs. (8) and (11) by expanding $j_0(qr)$ and $j_1(qr)$ to the first order in q. Then $\xi=0$ and v is proportional to q^2. One may also expect from Eq. (10) that the rate of changes in the absolute intensity of the π loss is three times of that of the σ loss [see Eq. (7)].

The strong dependence of the π loss on θ in comparison to the σ loss, provides us the opportunity to isolate the π loss by subtracting the integrated spectra taken at different θ. The integrated spectra are used because it is easier to normalize the integrated spectra to the same intensity for the σ loss before subtraction. For the highest sensitivity, the spectrum at $\theta=0°$ and at $\theta=70°$ are chosen. Shown in Fig. 4 is the difference spectrum. The data are given by the dots and the smooth lines represent the fitting of the data by two Gaussian functions, assuming that the major broadening is due to the instrument. The difference spectrum indicates that beside the main transition at 285 eV, there is a second, weaker transition in the π loss at 287.2 eV. It does not seem that the second transition is an artifact resulting from the subtraction procedure: it is not sensitive to the slight shift in the matching of the peak positions. A similar transition has also been observed by others,[1,3] although it has not been identified with the π loss.

Band calculations of graphite[18] have shown that the π band is rather flat near the Fermi energy E_f, and has a shallow minimum about 2 eV above E_f and at the zone

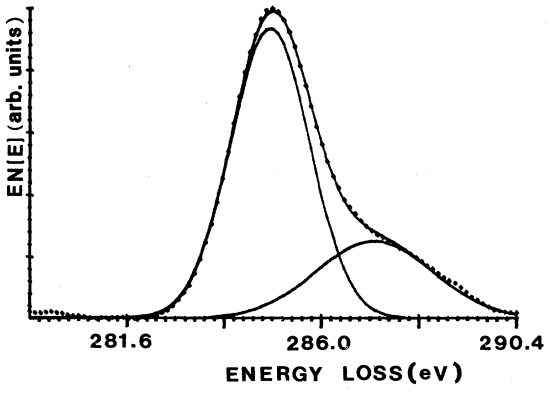

FIG. 4. The difference spectrum, given in $EN(E)$, between the integrated spectra at $\theta=0°$ and at $\theta=70°$.

face Q. This saddle point (labeled Q_{2g}^{-} in Ref. 18) leads to a Van Hove type of singularity in the density of states $\rho(E)$. Density-of-state calculations[14] have confirmed that there is a peak in $\rho(E)$ at the location corresponding to a loss energy $\sim$287.5 eV. We therefore assign the second π loss as the *direct* transition from the $C(1s)$ level to the saddle point Q_{2g}^{-} in the π band.

As discussed earlier, the loss peak at 285 eV is due to the formation of a π core exciton[14,17] near the Fermi level. The presence of the core exciton in the final state distorts the initial density of states $\rho(E)$ as indicated by the calculations of Mele and Ritsko. It is therefore important to realize that the presence of the core exciton does not exclude the direct transition to the saddle point Q_{2g}^{-}. The reason is that the core exciton is separated from the saddle point by more than 2 eV and the core exciton distorts only the density of states at the neighborhood of the resonance energy as given by the width of the resonance. To see this, we adopt the picture of the core exciton being a Fano-type resonance,[19] since the exciton is located within the conduction band. Let $\psi(E)$ be the unperturbed π-conduction state at energy E before the creation of the core hole. Then the creation of the core hole leads to the formation of a core exciton located at the resonance energy E_r. The configuration interaction between the core exciton and the unperturbed $\psi(E)$ leads to the final resonance state $\tilde{\psi}(E)$. Experimentally, we actually observe the transition from the $C(1s)$ level to $\tilde{\psi}(E)$ not from the $C(1s)$ level to $\psi(E)$. Denoting the excitation operator $\exp(i\mathbf{r}\cdot\mathbf{q})$ by T, the intensity of the π loss is given by

$$I(E)=|\langle 1s|T|\tilde{\psi}(E)\rangle|^2\rho(E)\ , \tag{12}$$

where $\rho(E)$ is the electron density of states of the unperturbed π-conduction band. We have dropped a numerical factor in Eq. (12) which depends on q^{-4}. At the energy-loss range concerned here, it is essentially constant. It has been shown[19] that

$$|\langle 1s|T|\tilde{\psi}(E)\rangle|^2=|\langle 1s|T|\psi(E)\rangle|^2[\Delta\Gamma/2+(E-E_r)]^2/[(\Gamma/2)^2+(E-E_r)^2]\ . \tag{13}$$

Γ is the width of the resonance state and $\pi\Delta^2/2$ is the ratio of the transition probabilities to the excitonic state and to a bandwidth Γ of $\psi(E)$ states. In the present case, $E_r\sim$285 eV and $\Gamma\sim$1 eV.[14] Substituting Eq. (13) into Eq. (12), we obtain

$$I(E)=|\langle 1s|T|\psi(E)\rangle|^2\rho_{\rm eff}(E)\ , \tag{14}$$

where

$$\rho_{\rm eff}(E)=\rho(E)\frac{[\Delta\Gamma/2+(E-E_r)]^2}{(\Gamma/2)^2+(E-E_r)^2}\ . \tag{15}$$

Thus $\rho_{\rm eff}(E)$ is the effective final density of states where the contribution from the core exciton is included. Two remarks are in order. First, from $\rho_{\rm eff}(E)$ we expect two peaks in $I(E)$. One peak is caused by the resonance in the curly bracket in Eq. (15) at $E=E_r$. The second peak originates from the Van Hove singularity in $\rho(E)$ due to the saddle point Q_{2g}^{-}. Since the saddle point Q_{2g}^{-} is more than 2 eV above the excitonic resonance, whose width is only about 1 eV, we expect that the direct transition to the saddle point would not have been obscured by the excitonic state. In general, $I(E)$ is dictated by the unperturbed (initial) density of states $\rho(E)$ when away from the resonance (i.e., $|E-E_r|\gg\Gamma/2$). However, near the resonance, the line shape is given by that of the exciton. Second, since both $\tilde{\psi}(E)$ and $\psi(E)$ have the same symmetry as the π orbital, the parameter Δ, as given by the ratio of the transition matrix elements from the $C(1s)$ level to these states, is independent of θ. Therefore, $\rho_{\rm eff}(E)$ is also independent of θ. The angular dependence of $I(E)$ is governed by $M_q(1s\rightarrow\pi)$, the transition matrix from the $C(1s)$ level to the unperturbed $\psi(E)$ state. This implies that if the energy loss at 287.2 eV is due to the direct transition to the saddle point Q_{2g}^{-} in the π band, it will have the same angular dependence as the energy loss at 285 eV due to the π exciton.

In summary, we have shown that there is a strong orientation dependence in reflection CEEL line shapes in anisotropic materials such as graphite. Detection with a cylindrical mirror analyzer does not remove this orientation dependence. The changes in the loss intensities as a function of the orientation indicate the breakdown of the dipole selection rule. There is significant contribution from the monopole transition from the $C(1s)$ level to the $2s$ orbital of the σ band. By taking the difference of spectra obtained at different orientations, a second transition in the π loss has also been identified.

[1]A. Koma and K. Miki, Appl. Phys. **A34**, 35 (1984).
[2]A. Koma and K. Yoshimura, Jpn. J. Appl. Phys. **22**, L173 (1983).
[3]L. Papagno and L. S. Caputi, Surf. Sci. **125**, 530 (1983).
[4]P. G. Lurie and J. M. Wilson, Surf. Sci. **65**, 476 (1977).
[5]L. Papagno, L. S. Caputi, M. De Crescenzi, and R. Rosei, Phys. Rev. B **26**, 2320 (1982).
[6]H. A. Bethe and R. Jackiw, in *Intermediate Quantum Mechanics* (Benjamin, New York, 1968), Chap. 17.
[7]R. Ludeke and A. Koma, Phys. Rev. Lett. **34**, 817 (1975).
[8]F. P. Netzer, G. Strasser, and J. A. D. Matthew, Phys. Rev. Lett. **51**, 211 (1983).
[9]J. J. Ritsko, N. O. Lipari, P. C. Gibbons, S. E. Schnatterly, J. R. Fields, and R. Devaty, Phys. Rev. Lett. **36**, 210 (1976).
[10]J. R. Fields, P. C. Gibbons, and S. E. Schnatterly, Phys. Rev. Lett. **38**, 430 (1977).
[11]L. A. Grunes and R. D. Leapman, Phys. Rev. B **22**, 3778 (1980).

[12]R. D. Leapman and J. Silcox, Phys. Rev. Lett. **42**, 1361 (1979).
[13]R. F. Willis, B. Fitton, and D. K. Skinner, J. Appl. Phys. **43**, 4412 (1972).
[14]E. J. Mele and J. J. Ritsko, Phys. Rev. Lett. **43**, 68 (1979).
[15]B. M. Kincaid, A. E. Meixner, and P. M. Platzman, Phys. Rev. Lett. **40**, 1296 (1978).
[16]J. Fink, T. Muller-Heinzerling, J. Pfluger, A. Bubenzer, P. Koidl, and G. Crecelius, Solid State Commun. **47**, 687 (1983).
[17]D. Denley, P. Perfetti, R. S. Williams, D. A. Shirley, and J. Stohr, Phys. Rev. B **21**, 2267 (1980).
[18]G. S. Painter and D. E. Ellis, Phys. Rev. B **1**, 4747 (1970).
[19]U. Fano, Phys. Rev. **124**, 1866 (1961).